Computed tomographic reconstruction based on x-ray refraction contrast

Anton Maksimenko[a)]
Graduate University for Advanced Studies (GUAS), Shonan International Village, Hayama, Miura, Kanagawa 240-0193, Japan

Masami Ando and Sugiyama Hiroshi
Graduate University for Advanced Studies (GUAS), Shonan International Village, Hayama, Miura, Kanagawa 240-0193, Japan and Photon Factory, Institute for Material Structure Science, KEK, Oho 1-1, Tsukuba, Ibaraki 305-0801, Japan

Tetsuya Yuasa
Faculty of Engineering, Yamagata University Yonezava, Yamagata 992, Japan

(Received 13 July 2004; accepted 8 February 2005; published online 17 March 2005)

Computed tomographic (CT) reconstruction technique is widely used in many fields of research. Commonly the CT-reconstruction is based on the x-ray absorption contrast. However, recently, methods for generating other x-ray contrasts have been developed. One of them is the refraction contrast which provides information on the deflection of the x-ray beam when penetrating through the object. This contrast has certain advantages and allows us to observe details invisible in the absorption images. Thus, CT based on the refraction contrast must have the same advantages. However, it requires a new mathematical algorithm and software. This letter is dedicated to the solution of the problem including theoretical consideration on the mathematical model which is the basis for the computer modeling and experimental realization of the technique. Actual experimental results together with the reconstructed images are presented and described. © *2005 American Institute of Physics*. [DOI: 10.1063/1.1891305]

The development of computed tomography (CT) in the early 1970's (Ref. 1) provided a powerful method for the nondestructive observations. Since that many CT modifications were invented and developed by numerous groups of researchers (see Refs. 2–5 for example). X-ray CT is now widely used in many field of science such as medical applications, material science, archaeology, and others. Most of them are based on the convenient absorption contrast because it iseasy to achieve and the reconstruction algorithms are well developed. However now other x-ray imaging contrasts are widely used (see Refs. 5–10). Among them, the so-called refraction contrast shows many advantages over the absorption contrast.[5,9–13] Although some attempts to make CT-reconstructions based on the refraction contrast are known,[3] none of them showed faithful representation of the object. So here we present the work which solves the problem.

When x-rays penetrate through an object, it deflects on the boundaries and inner structure so that the final deflection $\Delta\alpha$ can be expressed as follows:

$$\Delta\alpha = \int_S |\nabla \tilde{n}| \sin\phi \, ds, \tag{1}$$

where $\tilde{n}$ has a relation to the refraction index n as $\tilde{n}=1-n$, ϕ is angle between beam direction and gradient $\nabla\tilde{n}$. The integration is performed over the x-ray path S which can be approximated as a straight line taking into account the fact that $\tilde{n} \leqslant 10^{-5}$ in the x-ray region (see Ref. 14 for more details). The CT-reconstruction requires collecting information about the space distribution of deflection angles in different angular positions of the object. Thus, the final equation for the CT-reconstruction is

$$\Delta\alpha(\Theta,t)e^{i\Theta} = \int_S |\nabla \tilde{n}| e^{i\phi} ds. \tag{2}$$

Here Θ is rotation angle of the object and t is axis perpendicular to the x-ray beam as depicted in Fig. 1. The schematics of the CT-setup is shown in Fig. 1.

The mathematical formalism for solving the equation is similar to the one used for the absorption-based CT-reconstruction.[2] However Eq. (2) has a complex numerical form, which means that the present algorithms and software for absorption-based CT cannot be used. Moreover, Eq. (2) shows that the result the of reconstruction is the gradient of the refraction field while most users require a more realistic representation of the object which is the refraction index field itself rather than its gradient. For this purpose we developed a software which first reconstructs the vector field $\nabla\tilde{n}$ from the deflection angle distribution $\Delta\alpha(\Theta,t)$ and then builds the scalar field $\tilde{n}$. The gradient-to-field transformation

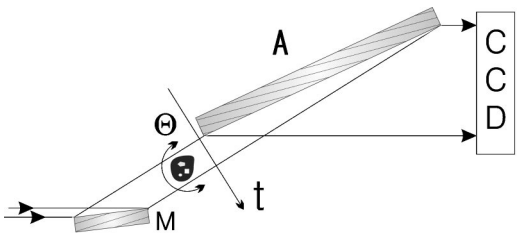

FIG. 1. Schematics of the experiment (view from above). Here M and A are monochromating and analyzing crystals, the object under investigation is the black body between them. The rotation axis for the CT scanning over Θ is perpendicular to the image plane.

[a)]Electronic mail: antonmx@post.kek.jp

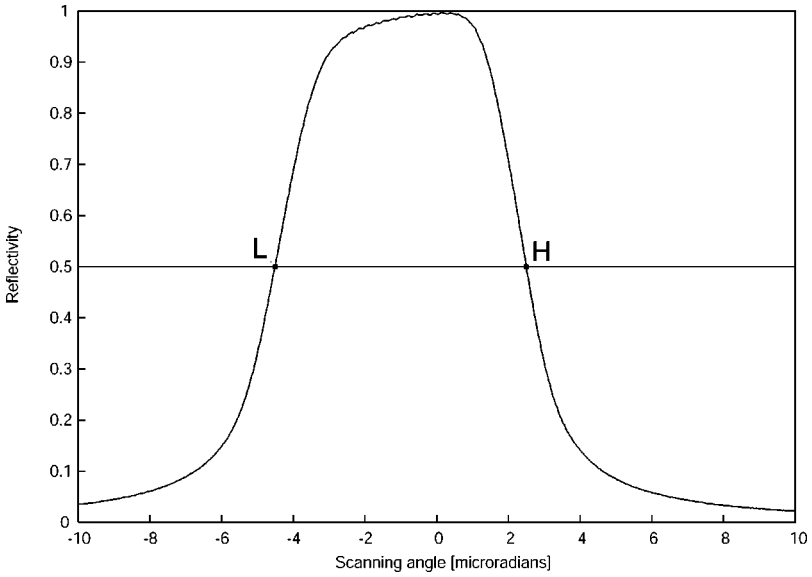

FIG. 2. Rocking curve of the analyzer. Series of images for reconstruction are taken in points L and H of the rocking curve. The reflectivity in both L and H points is 0.5.

$(\nabla\tilde{n}\rightarrow\tilde{n})$ is calculated accordingly to the property of the scalar field gradient

$$\tilde{n}(\mathbf{r}_0)=\int_{\mathbf{R}}^{\mathbf{r}_0}\nabla\tilde{n}(\mathbf{r})d\mathbf{r}, \tag{3}$$

where the starting point of the integration **R** can be placed anywhere on the boundary of the reconstructed image since the refraction index is assumed to be $(\tilde{n}\equiv 0)$ everywhere outside the object under investigation. In order todecrease the computational error in actual calculations we used the average value of four integrals starting in $(0,y_0)$, $(x_0,0)$, (T,y_0), and (x_0,T) [with T being the size of the reconstructed image and the pair (x_0,y_0) denoting the vector $\mathbf{r}_0$].

The problem of the experimental derivation of the function $\Delta\alpha(\Theta,t)$ is not obvious and different techniques were proposed by now.[5,9–13] The most reliable of them is the diffraction enhanced imaging (DEI) method presented in 1997.[11] The schematics of the experiment, performed in accordance with the DEI method, is presented in Fig. 1. The x-ray beam reflected from an asymmetrical monochromator *M*, pass through the object and, after reflection from the analyzer *A*, forms contrast which is acquired by CCD-camera. Photon energy used in experiment was 11.7 keV. Both monochromator and analyzer used Si (2 2 0) diffraction type and were asymmetrically cut with 9.5°. At these conditions Bragg angle $\Theta_B=16.0°$ and asymmetry factor $b=3.8$. The CCD-camera used had view area of $10.0(w)\times 7.5(h)$ mm with 1384×1032 pixels. The choice of the asymmetrically cut crystals is not mandatory and was done reasoning from the size of the object, view area of the CCD-camera and width of the rocking curve. All experiments were performed at the vertical wiggler beamline BL14B, at the Photon Factory, KEK, Japan. The rocking curve of the analyzer is shown in Fig. 2. In order to extract the refraction angle data in accordance with the DEI, one needs to take two pictures of the same object in two position of the analyzer. In Fig. 2 these positions are denoted as L and H. The refraction angle can be calculated according to Eq. 6(b) from Ref. 11. However, the theoretical model used in Ref. 11 utilizes the Taylor expansion of the rocking curve and therefore it is suitable only in limited ranges. In our experiments we used a slightly modified for the general case the DEI method was used in our experiment. These modifications consider the rocking curve of the analyzing crystal as is instead of its Taylor approximation.[15] The result of the refraction angle extraction is shown in Fig. 3. The sample presented in these figures is a fragment of the refill for the ball point pen deformed by fire. This sample was chosen because (i) it has no central symmetry, (ii) absorption contrast is low at 11.7 keV, (iii) it consists of different substances (plastic body with ink and air spaces inside). Figures 3(a) and 3(b) are original pictures in L and H positions of the analyzer, respectively. These images come with the corrected background (i.e., image with sample is divided by the background image without sample). The image in Fig. 3(c) shows extracted $\Delta\alpha$ proportional to the intensity of the gray scale with zero deflection corresponding to the middle gray.

Accordingly to the description above the refraction-based reconstruction process consists of the following steps:

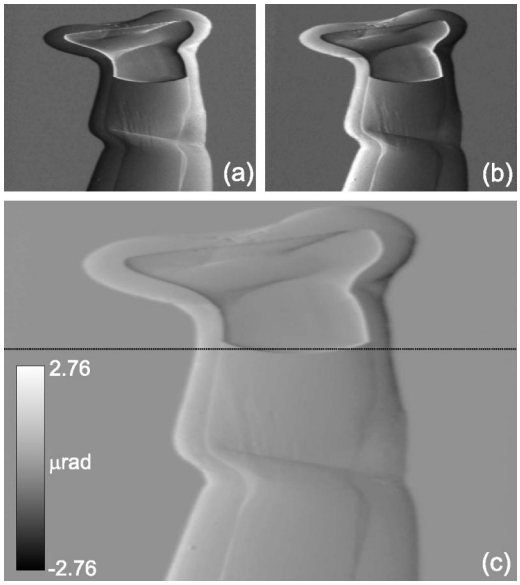

FIG. 3. Sample images taken in L (a) and H (b) positions of the analyzer and extracted from them deflection angle distribution $\Delta\alpha$ (c). Please note that the images (a) and (b) are presented with suppressed background. In (c) the dotted line shows slice which is presented in Fig. 4. All pictures have $2.6(w)\times 7.0(h)$ mm in size (the horizontal and vertical dimensions are of different scale due to the asymmetric reflection form the analyzer).

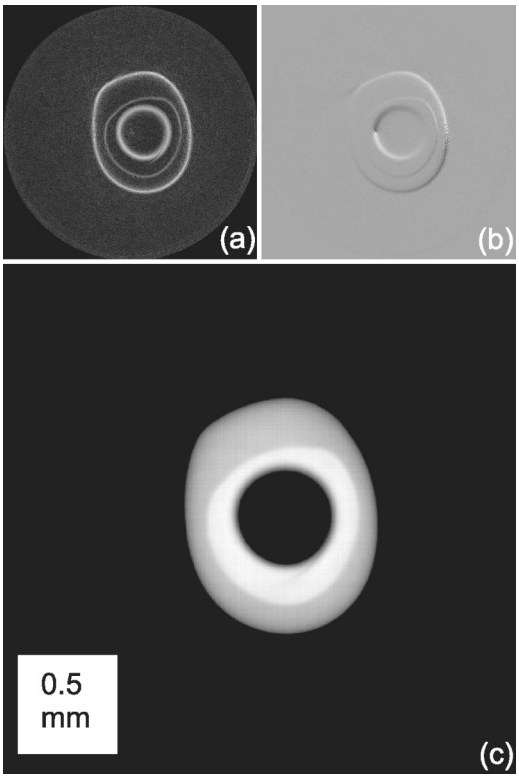

FIG. 4. Reconstructed $|\nabla\tilde{n}|$ (a), $|\nabla\tilde{n}|\sin\phi$ (b), and $\tilde{n}$ (c) in the slice marked in Fig. 3 with the dotted line. Size of every picture is 2.6×2.6 mm.

(i) Taking set of images at different $\Theta_m = m\Delta\Theta$ (with m an integer varying in ranges from 0 to M and $\Delta\Theta = 180°/M$) in the L point of the rocking curve [see Fig. 3(a)]. (ii) Taking the same set of images in the H point of the rocking curve [see Fig. 3(b)]. (iii) Extracting $\Delta\alpha(\Theta_m, t)$ from the sets accordingly to the modified DEI method [see Fig. 3(c) for extracted data]. (iv) CT-reconstruction on the base of Eq. (2). (v) Transformation of $\nabla\tilde{n}$ (which is the result of the CT-reconstruction) to more suitable $\tilde{n}$. Number of projections of the object in experiment was $M=360$ what gives $\Delta\Theta=0.5°$. Figure 4 shows reconstructed images of the slice marked in Fig. 3(c) with the dotted line numbered 410. This slice proves to be very interesting because it shows all three materials (plastic body, ink, air inside) in the region where the ink surface is curved by the surface tension. As it was mentioned above the reconstruction process output is the vector field $\nabla\tilde{n}$. It is shown in Figs. 4(a) and 4(b) as $|\nabla\tilde{n}|$ and $|\nabla\tilde{n}|\sin\phi$ correspondingly. Then the result of $\nabla\tilde{n}\Rightarrow\tilde{n}$ transformation is shown in Fig. 4(c). The 3D representation of the object is displayed in Fig. 5. They are *realistic* representation of the sample and all three substances are distinguishable in contrast. Please note that the refraction index of the ink proved to be larger than the one of the plastic body. This is because black ink is made using carbon black and has inclusions of pigments, such as titanium dioxide. One can note that the object on the reconstructed images has fuzzy edge. It

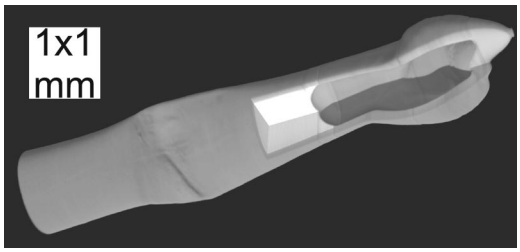

FIG. 5. Three-dimensional representation of the reconstructed object. The fragment of the reconstructed object was cut out to show the inner structure of the object. The ink can be easily distinguished due to its higher refractivity in comparison with the plastic body.

is the consequence of the x-ray optics limitations which appears mainly due to the Borrmann fan effect,[16] source size and the propagation-interference contrast.[5] We expect that the edge fuziness can be partially suppressed with the decrease of the object-to-detector distance (in our experiments it was 138 cm). One more artifact comes from $\nabla\tilde{n}\rightarrow\tilde{n}$ transformation and can be recognized as the netlike contrast of the pixel size in Fig. 4(c). It is possible to erase this unwanted contrast but it takes one order longer computation time and for most cases can be left as is since it does not distort the image strongly.

Finally, we can state that the problem of CT-reconstruction based on the refraction contrast was solved. The theory presented here was the base for the programming algorithm which was prepared and tested in experiments. Results of the reconstruction are shown and proven to be trustworthy.

[1] G. N. Hounsfield, Br. J. Radiol. **46**, 1016 (1973).
[2] A. C. Kak and Malcolm Slaney, *Principles of Computerized Tomographic Imaging* (IEEE, New York, 1988).
[3] F. A. Dilmanian, Z. Zhong, B. Ren, X. Y. Wu, L. D. Chapman, I. Orion, and W. C. Thomlinson, Phys. Med. Biol. **45**, 933 (1999).
[4] A. Momose, Nucl. Instrum. Methods Phys. Res. A **352**, 622 (1995).
[5] P. Cloetens, W. Ludwig, and J. Baruchel, Appl. Phys. Lett. **75**, 2912 (1999).
[6] T. J. Davis, D. Gao, T. E. Gureyev, A. W. Stevenson, and S. W. Wilkins, Nature (London) **373**, 595 (1995).
[7] T. J. Davis, T. E. Gureyev, D. Gao, A. W. Stevenson, and S. W. Wilkins, Phys. Rev. Lett. **74**, 3173 (1995).
[8] U. Bonse and M. Hart, Appl. Phys. Lett. **6**, 155 (1965).
[9] K. Hirano, A. Maksimenko, H. Sugiyama, and M. Ando, Jpn. J. Appl. Phys., Part 1 **41**, L595 (2002).
[10] A. Maksimenko, H. Sugiyama, K. Hirano, T. Yuasa, and M. Ando, Meas. Sci. Technol. **15**, 1251 (2004).
[11] D. Chapman, W. Thomlinson, R. E. Johnston, D. Washburn, E. Pisano, N. Gmuür, Z. Zhong, R. Menk, F. Arfelli, and D. Sayers, Phys. Med. Biol. **42**, 2015 (1997).
[12] V. Ingal and E. Beliaevskaya, J. Phys. D **28**, 2314 (1995).
[13] M. Ando, A. Maksimenko, H. Sugiyama, W. Pattanasiriwisawa, and K. Hyodo, Jpn. J. Appl. Phys., Part 1 **41**, 4742 (2002).
[14] A. Maksimenko, M. Ando, and T. Yuasa, in *Proceedings of the Joint Symposium on Bio-Sensing and Bio-Imaging 2001* (cd-rom edition, 2004), index of the paper on the CD: 1B-7.
[15] A. Maksimenko, M. Ando, H. Sugiyama, and K. Hirano (unpublished).
[16] G. Borrmann and K. Lehmann, *Crystallography and Crystal Perfection*, edited by G. N. Ramachandran (Academic, New York, 1963), p. 101.